

Supplementary Information for:

Tunable interchromophore electronic interaction of a merocyanine dye in hydrogen-bonded supramolecular assemblies scaffolded by bismelamine receptors

Shiki Yagai,* Masatsugu Higashi, Takashi Karatsu and Akihide Kitamura*

Experimental

Synthesis of bismelamines was reported previously.^{4c} Fluorescence quantum yields were estimated using Rhodamine 6G as a reference. Molecular modeling calculations were performed on MacroModel 9.0 using MMFF force-field method. Dynamic light scattering measurements were conducted on Beckmann Coulter N5 particle analyzer equipped with 25 mW He-Ne laser. Sample solutions were filtered with Millipore membrane filter (pore size = 0.2 μm) before measurements to remove dust.

Complexation between **1** and **M**

UV-vis titration experiment of monotopic melamine **M** (3×10^{-4}) with **1** (each addition is 3×10^{-5} , from 3×10^{-5} to 3×10^{-4} M) was carried out in MCH (Fig. S1a). Two spectral transition stages were clearly observed. First stage is hypsochromic shift of **1** from 465 nm to 461.5 nm (solid arrow in Fig. S1a), indicating the fully-complexed **1** (because of excess amount of **M**) to partially complexed **1**. This transition finished at the ratio of **M**:**1** = 2:1 (Fig. S1b), which clearly matches well with the stoichiometry based on the binding sites.

The second stage was observed at the ratio of **M**:**1** above 2:1, where the absorption band of **1** gradually broadened (dashed arrow in Fig. S1a). This indicates the presence of interchromophoric interaction. The spectral transition from 2:1 ($[\mathbf{1}] = 1.5 \times 10^{-4}$ M) to 2:1.2 ratio ($[\mathbf{1}] = 1.8 \times 10^{-4}$ M) is remarkable, again highlighting the 2:1 binding stoichiometry between **M** and **1**. At this stage, the stoichiometry of the binding sites mismatches (excess hydrogen-bonding sites in **1**), and the nonspecific association of complexes possessing free hydrogen-bonding sites (upper structures in Fig, S2), which have low solubility in apolar solvents, would occur in MCH.

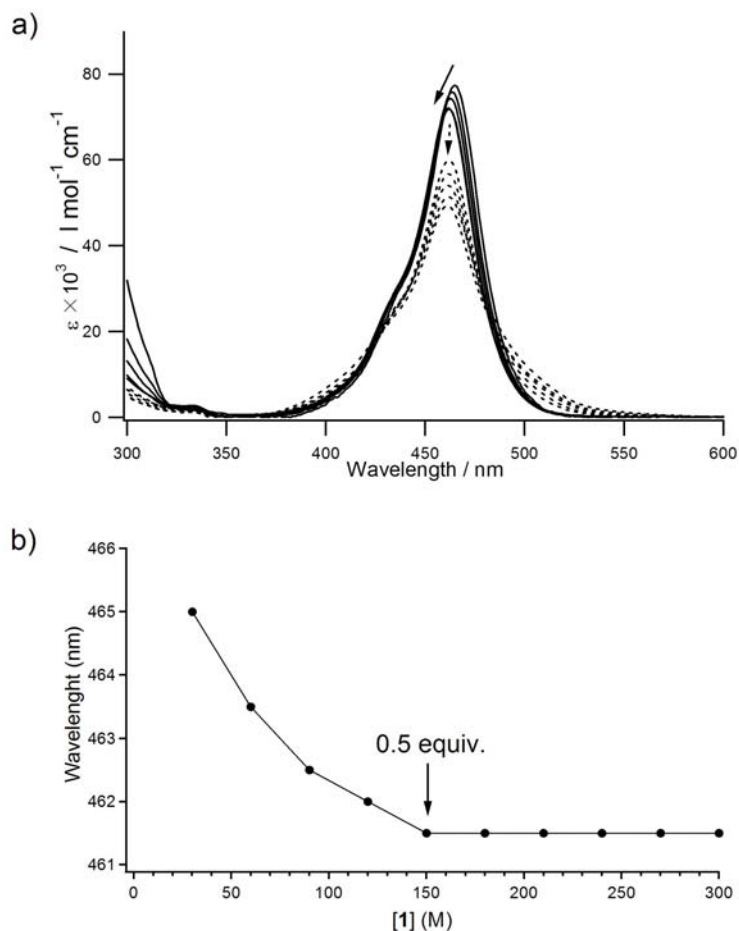


Fig. S1 (a) UV-vis titration of **M** (3×10^{-4}) with **1** (Solid line: 3×10^{-5} , 6×10^{-5} , 9×10^{-5} , 1.2×10^{-4} , 1.5×10^{-4} M; Dashed line: 1.8×10^{-4} M, 2.1×10^{-4} M, 2.4×10^{-4} M, 2.7×10^{-4} M, 3×10^{-4} M) in MCH. (b) Plot of the λ_{\max} of **1** with concentration.

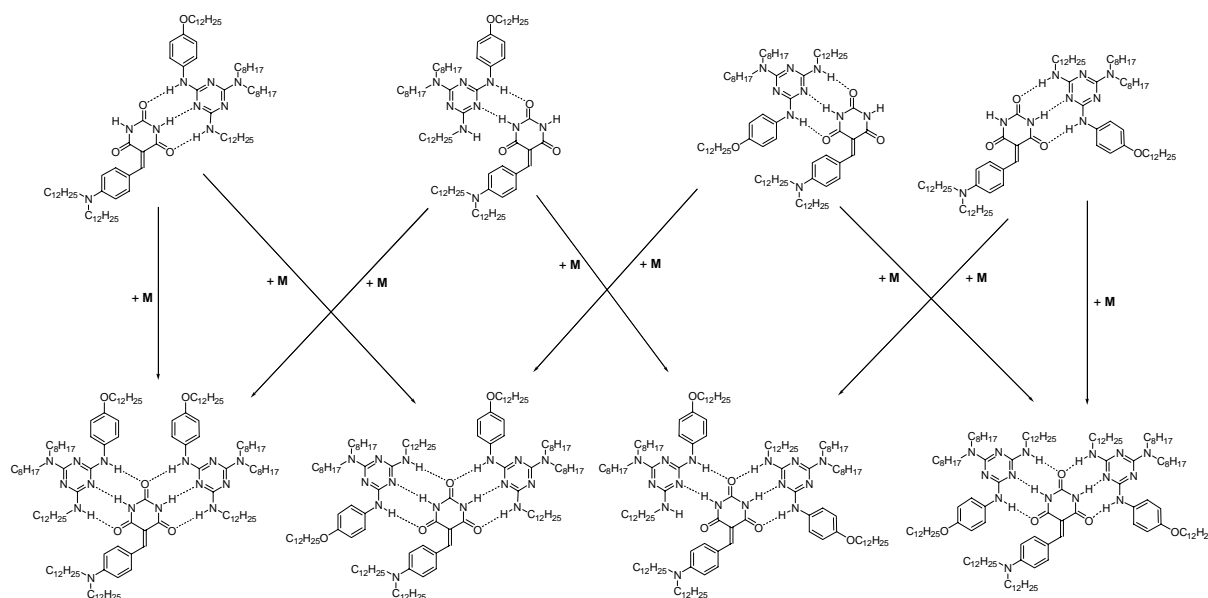


Fig. S2 Possible structures for 1:1 (upper) and 1:2 complexes (lower) of **1** and **M**.

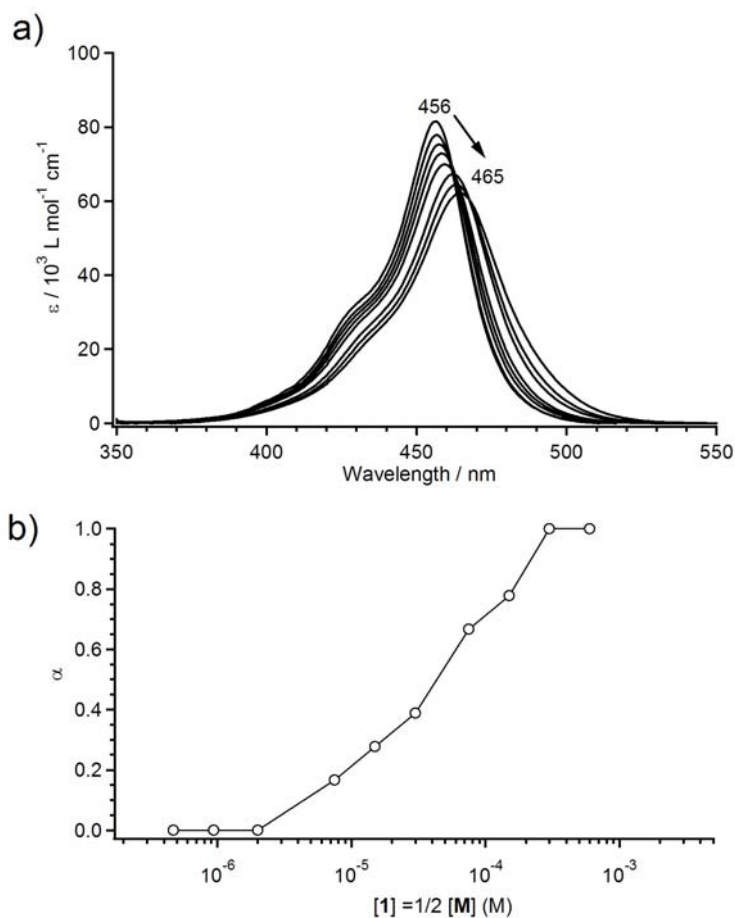


Fig. S3 (a) Concentration-dependent UV-vis spectra of **1** (2×10^{-6} to 3×10^{-4} M) in the presence of 2 equivalent of monotopic melamine **M**. Arrow indicates the changes upon increasing concentration. (b) Plot of the mole fraction of the complexed **1** versus the concentration obtained from the data shown in a).

Dilution experiments for **1/BM6** and **1/BM12**.

Stoichiometric mixtures of **1** and **BMs** were dissolved in MCH with various concentrations, and their UV-vis spectra were recorded. At low concentrations around 10^{-5} M, the mixtures of **1** and **BM12** and **1** and **BM6** showed absorption band at $\lambda_{\max} = 467$ nm, which can be attributed to the ICT band of the hydrogen-bonded **1** as observed in the case of monotopic **M**. When these mixtures were diluted up to 10^{-6} M at which the mixture of **1** and **M** exists as a monomeric blend (Figure 1b), the ICT bands persisted at $\lambda_{\max} = 467$ nm, indicating the formation of highly stable hydrogen-bonded assemblies. These assemblies can be assigned to the 1+1 closed species **1·BM** (Hamilton-type complex). For the mixture of **1** and **BM12**, the spectrum corresponding to the monomeric **1** ($\lambda_{\max} = 455$ nm) was obtained by dilution to 10^{-7} M, whilst the mixture of **1** and **BM6** showed the hydrogen-bonded spectrum ($\lambda_{\max} = 466$ nm) even at around the threshold concentration of our UV-vis measurement (5×10^{-8} M). This

result can be related to the stability of the 1+1 closed species depending on the length of the tether moiety of bismelamines ($n = 5$ is optimum length from molecular modeling calculations).

Fluorescence spectrum of 1/M.

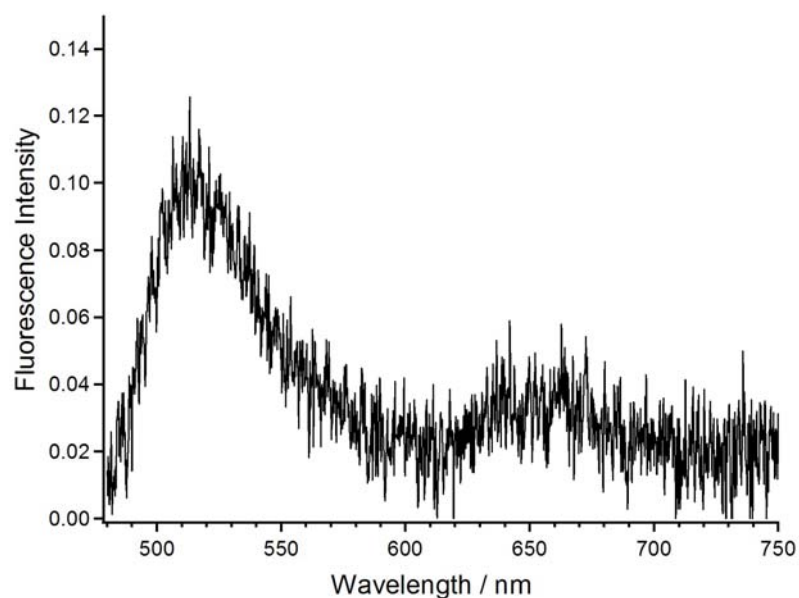


Fig. S4 Fluorescence spectra ($\lambda_{\text{ex}} = 460$ nm) of 1:2 mixture of **1** (1×10^{-4} M) and **M** (2×10^{-4} M).

Fluorescence excitation spectra of 1/BM3 and 1/BM6.

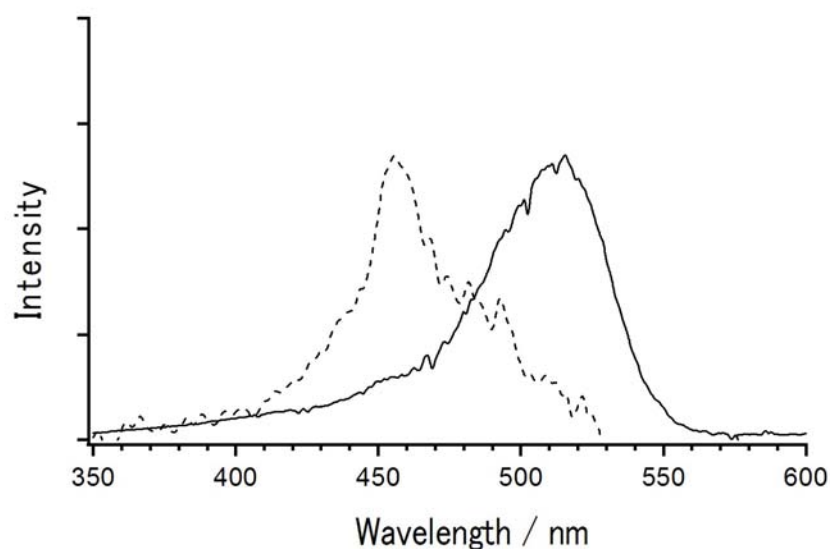


Fig. S5 Fluorescence excitation spectra of the mixture **1**–**BM3** (solid line: $[1] = [\text{BM3}] = 5 \times$

10^{-6} M, $\lambda_{em} = 550$ nm) and **1-BM6** (dotted line, $[1] = [BM6] = 2 \times 10^{-5}$ M, $\lambda_{em} = 615$ nm).

Molecular modeled structure of **1·BM6**

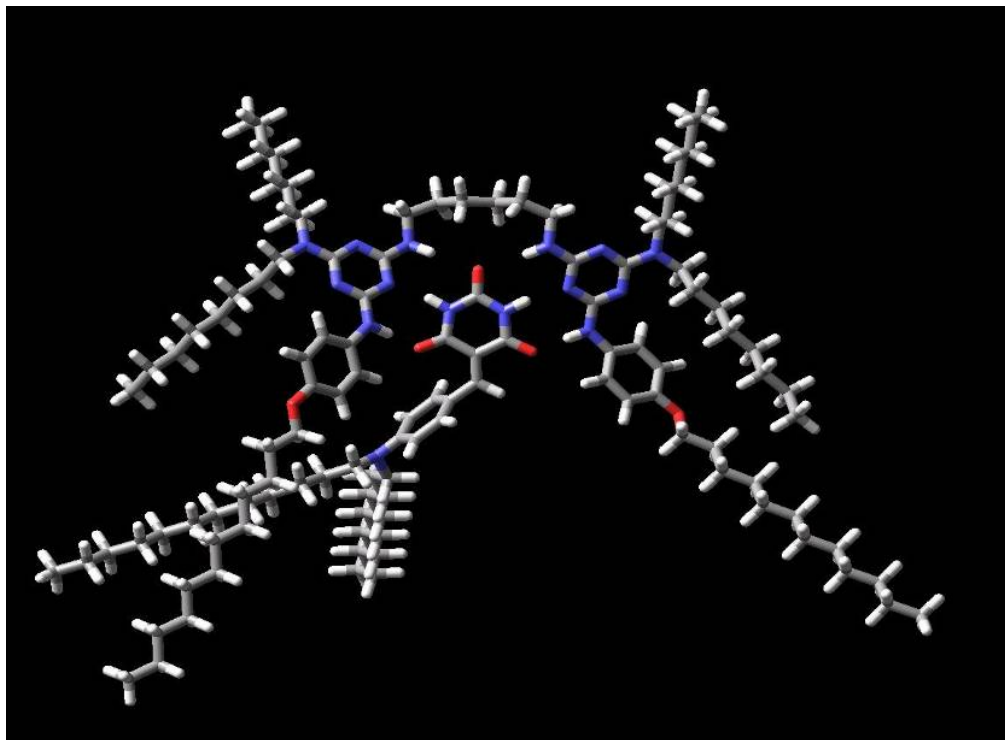


Fig. S6 Force-field energy-minimized structure of one stereoisomer of 1+1 closed species **1·BM6**.

¹H NMR spectra of the complexes

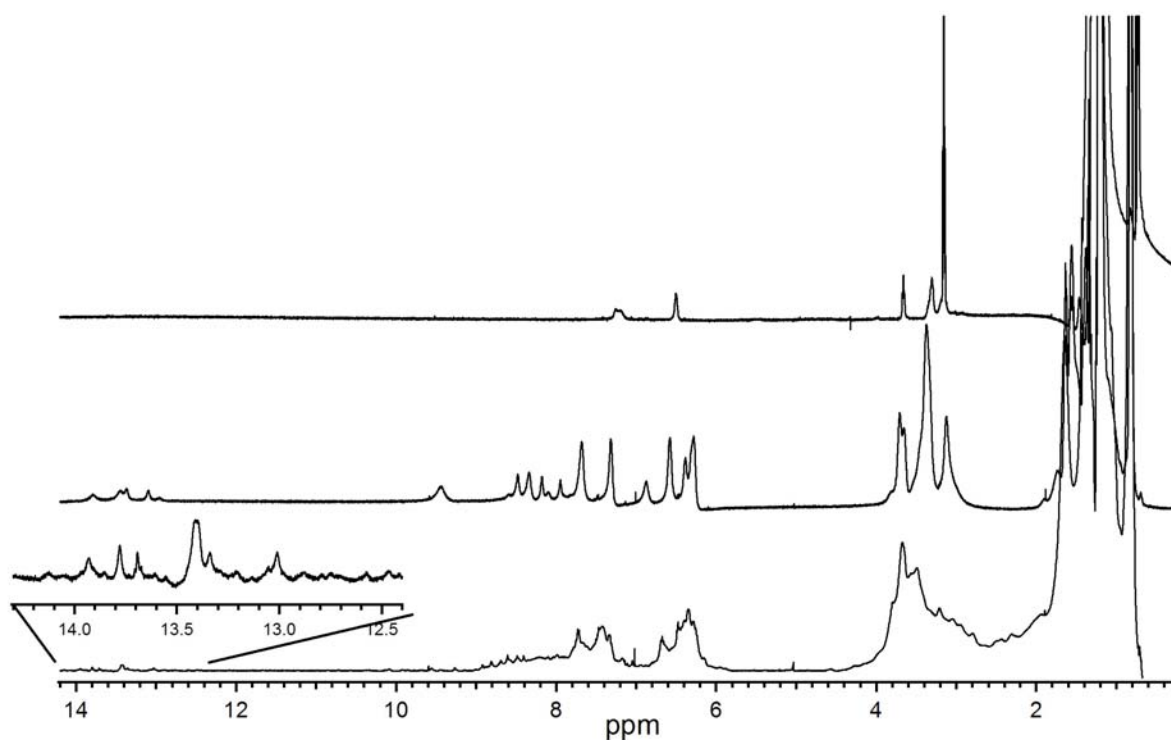


Fig. S7 ¹H NMR spectra of 1:1 mixtures of (bottom) **1-BM3**, (middle) **1-BM6**, (top) **1-BM12** in cyclohexane-*d*₁₂ ($[1] = [BM] = 5 \times 10^{-3}$ M).

For **1-BM6**, two sets of signals were observed. Molecular modelling calculation revealed that the 1+1 complex of **BM6** possesses axial chirality with respect to the twisting of two melamine plane, owing to the even carbon number of methylene spacer unit. Therefore, introduction of merocyanine dyes as guests induces four stereoisomers, two enantiomeric pairs of which can be detected by ¹H NMR (see Fig. S8). Detailed investigation in this aspect is under progress.

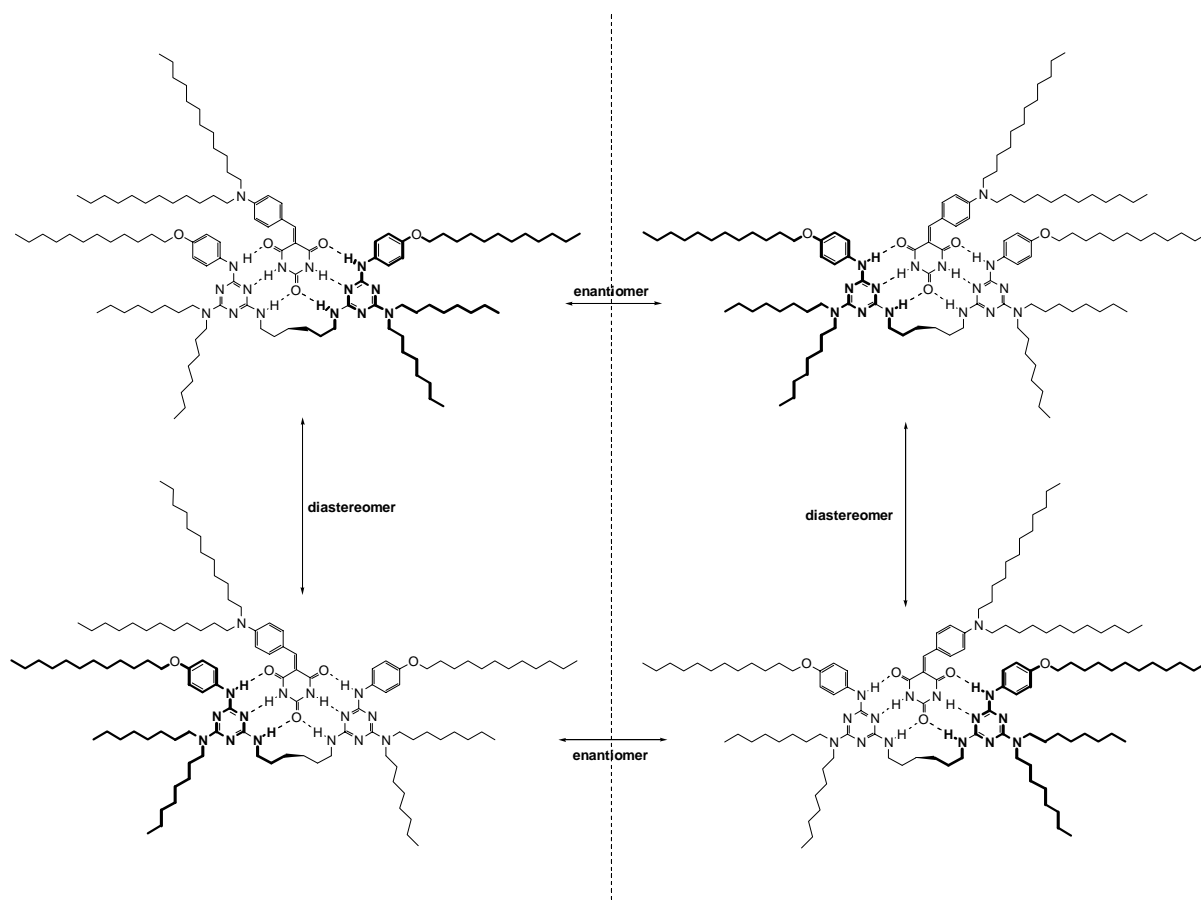


Fig. S8 Stereoisomers generated upon 1+1 complexation of **BM6** with **1**.